

Simulation and Control of MPPT Based Hybrid System with Boost Converter

J Barsana Banu¹, M Balasingh Moses² and S Rajarajacholan³

¹Research Scholar, University College of Engineering, BIT Campus, Tiruchirappalli, Tamilnadu, India.

²Assistant Professor, University College of Engineering, BIT Campus, Tiruchirappalli, Tamilnadu, India.

³Teaching Fellow, University College of Engineering, Anna University, Ariyalur Campus, Tamilnadu, India.

E-mail: barsanajamal@gmail.com

Abstract. A new topology of the hybrid (solar plus wind) power system with enhanced boost converter is proposed in this paper for standalone applications. The proposed hybrid power system comprises of solar panel and permanent magnet synchronous generator (PMSG) based wind turbine followed by rectifier and enhanced boost converter with resistive load. These natural sources deliver the load independently or concurrently depending on the requirement and accessibility of sources. The efficiency of the hybrid power system is increased by maximum power point operation. The most usually used Perturb and Observe (P&O) MPPT technique extracts the maximum power at the certain point. The complete structure was modelled and simulated in MATLAB/ SIMULINK package with variable solar irradiation and wind speed. The outcomes obtainable demonstrate the confirmation of the projected hybrid power system.

1. Introduction

Numerous inadequately occupied remote territories, stand-alone power system is necessary due to the low-power requirements, and it is too expensive to stretch out main power spread line to the remote territories. For instance, wind or solar power scheme can be used as individual or combined in nature to meet out the power requirement in such areas. Regardless, the characteristics of the renewable sources in general are dissimilar than the traditional power sources. The power production from these sources belongs to atmosphere conditions and is sporadic and/or fluctuating. Hence, hybrid power system is needed to fulfill the continuous load requirements. Among the various structures of hybrid system, photovoltaic and wind power systems are complimentary behavior to provide best outcomes. These natural sources are inconsistent due to its discontinuous availability. However, the system dependability can be developed by combining these two sources as a hybrid system as described in [1-3]. This hybrid system can be worked as either standalone or grid-connected operation depending upon the applications. The hybrid system is additional reliable for standalone system when PV-Wind energy system associated with battery storage is reported in [4-6]. The performance of PV-Wind-Diesel-Battery hybrid configuration is analyzed in [7]. Hybrid micro grid systems (wind/hydro/solar) likewise, created with MPPT strategies [8, 9] and the distinctive technique for controlling the wind turbine speed in a micro grid is depicted in [10] yet it needs an excellent speed sensor. The broad review of the different optimum sizing procedures and optimization criteria of the hybrid power system in perspective of small PV, wind, hydro and storage devices is reported in [11]. The power output developed from RES such as PV and wind power system is unreliable because of changing



every time to time. MPPT controller can be used to get the maximum power obtainable from the two natural sources. Various MPPT procedures are given in the literature. Among them perturb and observe MPPT technique is widely utilized because of simple structure. The paper [12] comprises of solar and DFIG driven wind hybrid system with boost converter. This system requires three distinct controllers such as MPPT controller utilized alone for PV; DFIG needed rotor and grid side controller with special converter and control circuit to regulate the voltage and rotor speed. An topology of PV-wind PMSG hybrid generator is proposed [13] with two low price controllers like MPPT and hysteresis controllers, which are working independently to regulate the duty cycle of the DC-DC converter and the inverter for extracting the most extreme power from the solar and wind power system. These papers [12] and [13] required two additional controllers. During the power scarcity by the hybrid system, a battery bank is needed to satisfy the load demand as suggested in [14] still it needs a complicated vector control method in addition with solar and wind MPPT controllers.

By using fuzzy rules, duty cycle of the boost converter is generated to track the maximum power for both solar and wind power system individually. Hence, the reliability of the HPS can be enhanced by the closed-loop system is reported in [15]. In the paper [16], PV-wind, energy has been coordinated together utilizing the combination of CUK-SEPIC converters, CUK converter is operated by the solar cell and SEPIC converter works under wind turbine. Therefore, this methodology has suggested rather than the conventional converter techniques to reduce current harmonics. The soft switching dc-dc converter discussed in [17] is incorporated with wind-PV hybrid configuration is proposed in this paper. The simulation of wind- PV with common MPPT controller is utilized to control the power devices of the enhanced boost converter to extract MPP are done in MATLAB. Results are investigated by varying contribution parameters such as irradiation level, temperature for solar source and wind speed for wind turbine. The modeling of solar, wind sources and PMSG are described in detail. The simulation results reveal the confirmation of the proposed hybrid power system suitable for standalone applications.

2. The proposed hybrid configuration

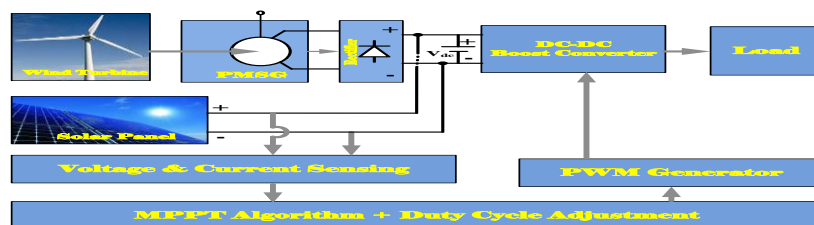


Figure 1. Outline configuration of the proposed hybrid power system

Figure.1 illustrates the configuration of the proposed hybrid power configuration. The proposed hybrid power system contains solar panel with parallel and series connected cells, Permanent magnet synchronous generator(PMSG) driven wind turbine, Rectifier, DC-Dc boost converter and MPPT controller. Rectifier receives AC input from PMSG via wind turbine depending upon wind speed, pitch angle, and converts this AC in to DC. Then the output from the solar panel and rectifier is synchronously connected to boost converter to boost the voltage gotten from the rectifier. MPPT controller sense voltage and current from the rectifier and control the duty ratio of the switch used in the proposed boost converter. The operation technique proposed in this study is gone for reducing the utilization of fossil fuel and attractive the use of renewable energy sources (RES).

3. PV module modeling

A solar cell is made up of the semiconductor device, which transfer solar energy into electrical energy. Solar array is made up of the number of parallel and serious connected solar cells. A generic identical

circuit as shown in figure.2 represents the solar module consists of the single diode with series R_s and parallel resistance R_p .

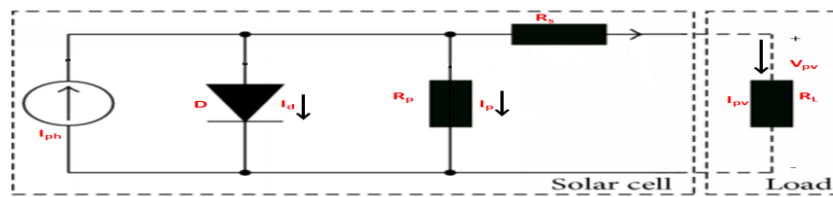


Figure 2. Equivalent circuit of PV module

The four variables required for this model are the two input variables, sunlight based radiation E_G (W/m^2) and surrounding temperature T_a ($^{\circ}C$), and the two output terminal variables, PV cell current I_{pv} (A) and voltage V_{pv} (V). According to KCL, the PV cell current (I_{pv}) is expressed by.

$$I_{pv} = I_{ph} - I_d - I_p \tag{1}$$

Where, I_{ph} is the Photo current; I_d is the Diode current; I_p is the Shunt current.

$$I_{pv} = \left[I_{sc} + K_i (T - T_r) \right] \frac{S}{100} - I_0 \left[e^{\frac{q(V_{pv} + I_{pv}R_s)}{AKT}} \right] - I_p \tag{2}$$

Where I_{sc} is the Short circuit current at T_r ; K_i is the temperature coefficient of short circuit current; S is the Global solar radiation in mW/cm^2 . The module immersion current (I_0) changes with cell temperature, which is communicated as,

$$I_0 = I_{sotr} \left(\frac{T}{T_r} \right)^3 e^{\frac{qE_G}{KA} \left(\frac{1}{T_r} - \frac{1}{T} \right)} \tag{3}$$

Where, E_G is the Band gap energy; T_r is the Reference temperature = 301.18 K; T is the Cell temperature. The module's reverse immersion current (I_{sotr}) and the Shunt current I_p is given by.

$$I_{sotr} = \frac{I_{sc}}{e^{\left(\frac{qV_{oc}}{N_{ss}AKT} \right)}} \tag{4},$$

$$I_p = \left(\frac{V_{pv} - I_{pv}R_s}{R_p} \right) \tag{5}$$

The output current obtained from the PV module (I_{pv}) is given by.

$$I_{pv} = N_{pp} I_{ph} - N_{pp} I_0 e^{\left[\frac{q(V_{pv} + I_{pv}R_s)}{N_{ss}AKT} \right]} - 1 \tag{6}$$

Where, N_{pp} is the Quantity of parallel cells; N_{ss} is the Quantity of series cells, q = electron charge (1.6×10^{-19} C); V_{oc} = open-circuit voltage (V) of the PV board; k = Boltzmann's constant with the quality 1.3805×10^{-23} J=K; A = ideality variable with the worth 1.2; I_0 = PV module immersion current (An); The power extracts from the PV array can be estimated by the subsequent equation.

$$P = N_{pp} I_{ph} V_{pv} - N_{pp} I_0 V_{pv} \left(e^{K_0 \left(\frac{V_{pv} + I_{pv}R_s}{N_{ss}} \right)} - 1 \right) - \frac{V_{pv}}{R_p} \left(\frac{V_{pv}}{N_{ss}} + IR_s \right) \tag{7}$$

The temperature (T) of a PV cell is spoken by.

$$T = 3.12 + 0.25S + 0.899T_a - 1.3W_s + 273 \tag{8}$$

Where, T_a is the ambient temperature; W_s is the Wind speed; S is the solar radiation. In the scientific model, number of parallel and serious connected cells are $N_{ss} = 36$ and $N_{pp} = 2$.

4. Wind turbine model

The overall characteristic of the wind turbine is described by the non-dimensional curve i.e. coefficient of performance (C_p) versus tip-speed ratio λ . It is given by equation (9)

$$C_p(\lambda) = 0.043 - 0.108\lambda + 0.146\lambda^2 - 0.0602\lambda^3 + 0.0104\lambda^4 - 0.0006\lambda^5 \quad (9)$$

The tip-speed ratio is specified by the expression:

$$\lambda = \frac{R\omega_m}{V_w} \quad (10)$$

Where, R is the rotor radius of the wind turbine in m, ω_m is the rotor angular speed in rad/sec. and V_w is the wind velocity in m/s. The power output of wind turbine P_t is measured utilizing equation (3) as:

$$P_t = 0.5C_p(\lambda)AV_w^3 \quad (11), \quad Pt = Tt\omega_m \quad (12)$$

Where, A is the rotor swept area of wind turbine. Combining equations (9), (11) and (12), the expression for torque T_t created by the wind turbine is expressed as:

$$T_t = 0.5rAR \frac{C_p(\lambda)}{\lambda} V_w^2 \quad (13)$$

The power obtained from the wind is more extreme at maximum C_p . This happens at a characterized estimation of the tip speed proportion. Consequently, for every wind speed; there is an ideal rotor speed where greatest power is extricated from the air. In this way, if the wind velocity is thought to be steady, the estimation of C_p relies upon the wind turbine rotor speed. In this manner, by controlling the rotor speed, the power output of the turbine is controlled.

5. PMSG modeling

WECS can be utilized together synchronous and induction generators depending upon the requirement. Changeable speed permanent magnet synchronous generator (PMSG) is broadly utilized as a part of wind energy systems as it has maximum efficiency, weight less, simple maintenance, easy control and no requirement for magnetizing and reactive current. The gearbox present in the changeable speed wind turbine creates additional cost and maintenance. Utilizing direct driven PMSG enhances reliability as well as reductions weight in the nacelle. The PMSG is modeled using d-q synchronous reference frame. The voltage equations are described below

$$V_d = -R_s i_d - L_d \frac{di_d}{dt} + \omega L_q i_q \quad (14), \quad V_q = -R_s i_q - L_q \frac{di_q}{dt} - \omega L_d i_d + \omega \lambda_m \quad (15)$$

The electronic torque is specified as

$$T_e = 1.5\rho \{ \lambda i_q + (L_d - L_q) i_d i_q \} \quad (16)$$

$$\begin{bmatrix} V_{qs} \\ V_{ds} \\ V_{qr} \\ V_{dr} \end{bmatrix} = \begin{bmatrix} R_s + \rho L_s & 0 & PL_m & 0 \\ 0 & R_s + \rho L_s & 0 & PL_m \\ PL_m & -\omega_r L_m & R_r + \rho L_r & -\omega_r L_r \\ \omega_r L_m & PL_m & \omega_r L_r & R_r + \rho L_r \end{bmatrix} \begin{bmatrix} i_{qs} \\ i_{ds} \\ i_{qr} \\ i_{dr} \end{bmatrix} \quad (17)$$

Where, L_d and L_q are direct and quadrature axis inductances, i_d and i_q are straight and quadrature axis currents, V_d and V_q are direct and quadrature axis voltages, ω_r is the rotor angular velocity, λ is amplitude of flux induced and p is number of set of poles. If there is a squirrel cage induction generator (SCIG), dynamic modeling is done by stationary d-q reference frame accompanying with the following expression. The expressions of stator side are

$$\lambda_{ds} = L_s i_{ds} + L_m i_{dr} \quad (18), \quad \lambda_{qs} = L_s i_{qs} + L_m i_{qr} \quad (19)$$

$$L_s = L_{ls} + L_m \quad (20), \quad L_r = L_{lr} + L_m \quad (21)$$

$$V_{ds} = R_s i_{ds} + \frac{d}{dt} \lambda_{ds} \quad (22), \quad V_{qs} = R_s i_{qs} + \frac{d}{dt} \lambda_{qs} \quad (23)$$

The expressions of rotor side are

$$\lambda_{dr} = L_r i_{dr} + L_m i_{ds} \quad (24), \quad \lambda_{qr} = L_r i_{qr} + L_m i_{qs} \quad (25)$$

$$V_{dr} = R_r i_{dr} + \frac{d}{dt} \lambda_{dr} + \omega_r \lambda_{qr} \quad (26), \quad V_{qr} = R_r i_{qr} + \frac{d}{dt} \lambda_{qr} - \omega_r \lambda_{dr} \quad (27)$$

The equations of the gap flux linkages are

$$\lambda_{dm} = L_m (i_{ds} + i_{dr}) \quad (28), \quad \lambda_{qm} = L_m (i_{qs} + i_{qr}) \quad (29)$$

Where, R_s and R_r are stator and rotor winding resistances, L_m is the magnetizing inductance, L_{ls} and L_{lr} are stator and rotor leakage inductances, ω_r is the angular speed of the electrical rotor, i_d and i_q are straight and quadrature axis currents, V_d and V_q are direct and quadrature axis voltages, λ_d and λ_q are direct and quadrature axis fluxes. The power output and the turbine torque (T_t) in expression of rotational speed can be gotten by substituting (17) in (16)

$$P_w = 0.5 \rho A C_p (\lambda, \beta) \left(\frac{R \omega_{opt}}{\lambda_{opt}} \right)^3 \quad (30)$$

$$T_t = 0.5 \rho A C_p (\lambda, \beta) \left(\frac{R}{\lambda_{opt}} \right)^3 \omega_{opt} \quad (31)$$

The power coefficient (C_p) is a nonlinear function communicated by the fitting condition is given by

$$C_p = 0.5176 \left(\frac{116}{\lambda_i} - 0.4\beta - 5 \right) e^{\frac{-21}{\lambda_i}} + 0.0068\lambda \quad (32)$$

With,

$$\frac{1}{\lambda_i} = \frac{1}{\lambda + 0.08\beta} - \frac{0.035}{\beta^3 + 1} \quad (33)$$

6. Three-phase diode rectifier

The 3Φ Full bridge rectifier can be coupled straight to the three-phase source to rectify the generated output voltage from the PMSG. The output dc voltage across the rectifier is

$$V_{dc} = (3\sqrt{2}/\pi) V_L \quad (34)$$

Where V_{dc} is output DC voltage across the rectifier and V_L is the input ac voltage from PMSG.

7. DC-DC boost converter

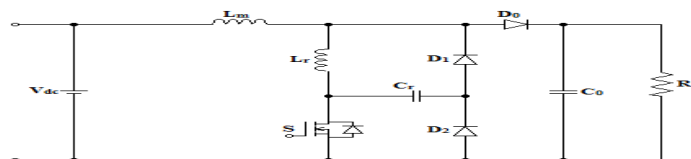


Figure 3. Boost converter used in the hybrid system

Figure.3 shows the recently proposed improved dc-dc converter with LCD snubber configuration for battery applications [17]. The circuit [17] is introduced to attain high efficiency and reduces switching losses. The unregulated DC voltage from the diode rectifier is known as input to the developed DC-DC boost converter shown in fig.3. The rectifier output voltage will change due to variations in wind speed. Improved DC-DC boost converter is needed to obtain the regulated dc voltage output as well as to realize the MPPT operation. A single power switch S is needed, which reduces the cost and simplifies the control over the system. For ease, a resistance load R_L is linked directly to the output from the boost converter to consume the power generated by the WECS. The output voltage of the boost converter is given by

$$\frac{V_0}{V_{dc}} = \frac{1}{1-D} = \frac{I_{dc}}{I_0} \tag{35}$$

The control algorithm uses only the dc-link voltage $V_{dc}(t)$ and the dc-current $I_{dc}(t)$ measurements to adjust directly the duty cycle D.

8. MPPT implementation

To enhance the efficiency of the hybrid power system MPPT is implemented to shift the working voltage nearest to the most extreme power under varying weather conditions. Among the various configurations of MPPT, Perturb and observe algorithm is applied in this paper as shown in figure.4. This is simple and admired method. The procedure is given below.

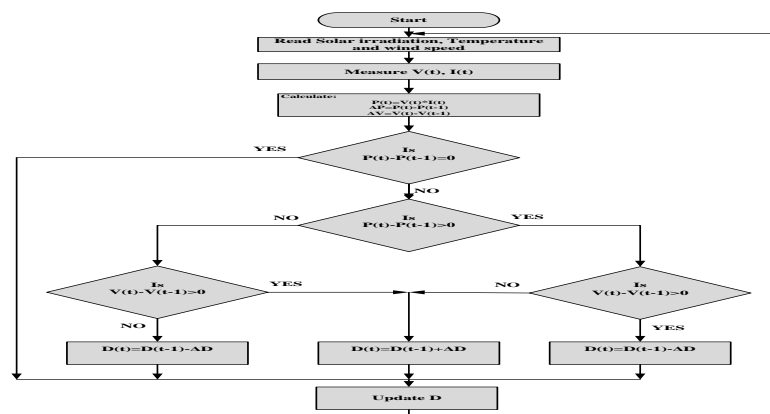


Figure 4. The flowchart of perturb and observe (P&O) MPPT technique

Step1: Read the input parameters of the hybrid system such as solar irradiation, ambient temperature and wind speed.

Step2: Measure the solar panel voltage and current, which are same as that of the diode rectifier voltage and current.

Step 3: The voltage $V(t)$ and $I(t)$ are given as input to the MPPT controller and compute the Power, $P(t) = V(t)*I(t)$.

Step 4: After the power, $P(t)$ is obtained and perturbing the duty ratio of the boost converter switch (increment or decrement) to vary the operating point of the system (perturb $V(t)$ and $I(t)$) and the difference between Present and previous values of power is computed by $\Delta P = P(t) - P(t-1)$.

Step 5: Then the power increases with voltage increment; the operating point of the system is shifting towards the most extreme power point. Hence, the size of the perturbation is positive or left constant. The mathematical expressions are,

$$\Delta P / \Delta V > 0; \quad D(t) = D(t-1) + \Delta D \text{ and } \Delta P / \Delta V < 0; \quad D(t) = D(t-1) - \Delta D$$

Step 6: Next the power decreases with voltage decrement; the operating point of the system is shifting away from the most extreme power point. Hence, the size of the perturbation is return back and pushes the system to be operating in the reverse MPP.

Step 7: The MPPT controller generates the desired duty ratio for the boost converter.

Step 8: This procedure is frequent awaiting the MPP is achieved.

9. Results and discussions

A solar-wind hybrid power system with Common MPPT control has been simulated with MATLAB environment, and the results are presented here. The solar panel and wind turbine parameters for 20 m/s wind speed and 1500 W/m² irradiation are appeared in the table 1. As per solar irradiation and temperature level, the dc voltage obtained from PV panel changes time to time similarly as per variation in the wind speed and pitch angle, the ac output voltage obtained from wind turbine via the permanent magnet synchronous generator fluctuates as shown in Figure.5.

Figure. 6 shows the simulated results of the hybrid system at the wind speed of 20m/s at 1500 W/m² and pitch angle =0°. Figure. 6. (A) and Figure. 7. (A) Demonstrates the voltage and power obtained from the rectifier side. Up to 0.52 sec the system receive energy from wind turbine and after 0.52 sec the system collects energy from solar panel. Figure 6.(B) and Figure 7.(B) illustrates the voltage and power acquired from the dc-dc boost converter. It clearly shows that voltage doubles at every second with respect to rectifier voltage and power losses slightly than the rectified power. From this, we reach the efficiency of the boost converter by 93%.

Table.1.Parameters of hybrid system

Source	Parameters	Values
Wind turbine	Input(Wind speed)	20 m/s
	Maximum Power	1600 W
	Pitch angle	0
	Base wind speed	10 m/s
Solar Panel	Input(Irradiation and Temperature)	1500 W/m ²
	Maximum power	400 W
	Number of series cells	36
	Number of parallel cells	2
	Input voltage	80-180 V
Boost Converter	Output voltage	160-360 V
	Output power	380-1500W
	Switching frequency	50 KHZ

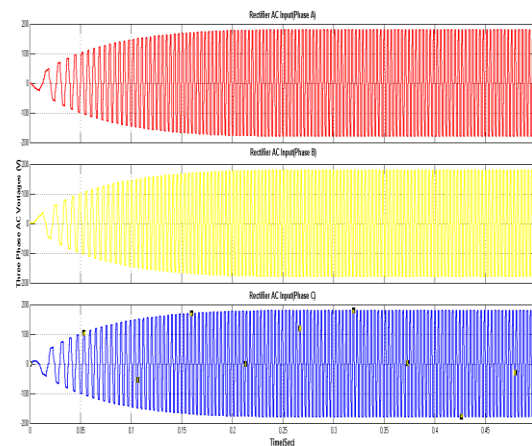


Figure 5. Three Phase AC Voltage generated by PMSG.

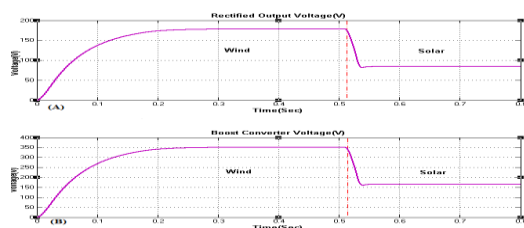


Figure 6. Simulated voltage results for wind speed 20m/s at 1500 W/m² and pitch angle =0° (A) Rectified DC output Voltage (B)

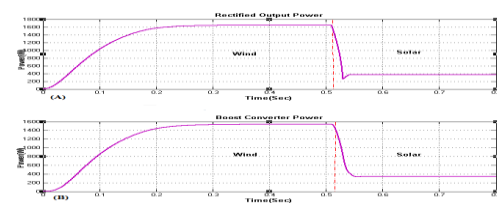


Figure 7. Simulated power results for wind speed 20m/s at 1500 W/m² and pitch angle =0° (A) Rectified output power

Boost converter voltage.

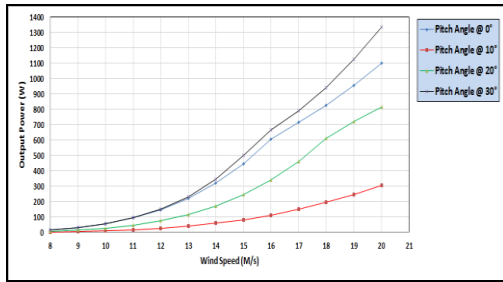


Figure 8. Maximum-power tracking concerning the assortment in the wind speeds at the different pitch angle.

(B) Boost converter power.

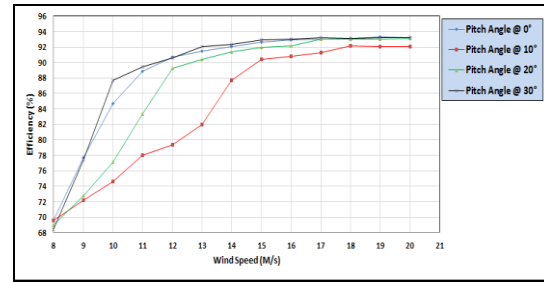


Figure 9. Tracking efficiency concerning the assortment in the wind speeds at different pitch angle.

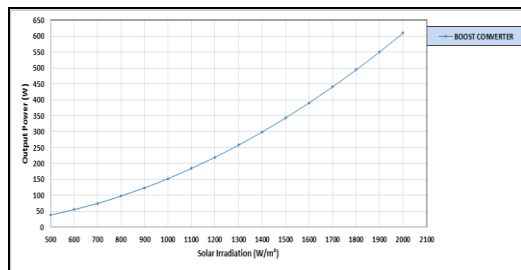


Figure 10. Maximum-power tracking concerning the assortment in the solar irradiation at constant temperature and fixed wind speed.

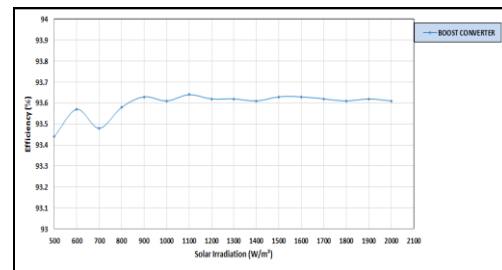


Figure 11. Tracking efficiency concerning the assortment in the solar irradiation at constant temperature and fixed wind speed.

Figure. 8 and figure. 9 depicted the maximum-power tracking and tracking efficiency of the hybrid system concerning the assortment in the wind speed at the different pitch angle. It is observed that the proposed hybrid system tracks maximum power at a pitch angle 30° . Figure. 10 and figure. 11 shows the maximum power tracking and tracking efficiency of the hybrid system in regard to the assortment in the solar irradiation at constant temperature and fixed wind speed and saw that the power increases with an irradiation level.

10. Conclusion

The MPPT based solar-wind hybrid energy system with boost converter is studied in this paper. To increase the conversion efficacy of the suggested standalone hybrid system, an MPPT algorithm is utilized. Perturb and observe algorithm is used to provide the required duty ratio to control the boost converter with unpredictable weather conditions. A detailed analysis of solar, wind and PMSG modeling has been done in this work. The proposed system is simulated in MATLAB/ SIMULINK environment under varying solar irradiation, wind speed and temperature and these results showed that the conversion efficiency reaches around 93%. According to the overall discussion, it could be inferred that the proposed hybrid system is the suitable choice for standalone applications.

11. References

[1] Subhadeep B and Shantanu A 2015 PV-wind hybrid power option for a low wind topography *Energy Conversion and Management*. **89** pp 942–954.
 [2] Chih-Lung S, Tsair-Chun L, Siou-Hong Z and Su-Wen W 2015 Voltage Gain Derivation Based on Energy-Balanced Criterion for a Novel Hybrid-Input PV-Wind Power Conversion System *Hindawi Publishing Corporation Mathematical Problems in Engineering*. <http://dx.doi.org/10.1155/2015/623161>(2015).

- [3] Bhave A G 1999 Hybrid solar-wind domestic power generating system-a case study *Renewable Energy*. **17** pp 355-358.
- [4] Naveen kumar R and Baskaran J 2014 Energy Management system for Hybrid RES with Hybrid Cascaded Multilevel inverter *International Journal of Electrical and Computer Engineering (IJECE)*. **4** pp.24-30.
- [5] Cheng-Wei C, Chien-Yao L, Kun-Hung C and Yaow-Ming C 2015 Modeling and Controller Design of a Semiisolated Multiinput Converter for a Hybrid PV/Wind Power Charger System *IEEE Transactions on Power Electronics*. **30** pp. 4843-4853.
- [6] Bogdan S. borowy and Ziyad M. salameh 1996 Methodology for Optimally Sizing the Combination of a Battery Bank and PV Array in a Wind/PV Hybrid System *IEEE Transactions on Energy Conversion*. **11** pp. 367-375.
- [7] Fazia B, Kamal M, Said D and Omar Behar 2015 Feasibility study and energy conversion analysis of stand-alone hybrid renewable energy system *Energy Conversion and Management*. **105** pp. 471-479.
- [8] Binayak B, Shiva raj P, Kyung-Tae L and Sung-Hoon A 2014 Mathematical Modeling of Hybrid Renewable Energy System: A Review on Small Hydro-Solar-Wind Power Generation *International Journal of Precision Engineering and Manufacturing-Green Technology*. **1** pp. 157-173.
- [9] Szeidert I, Filip I and Prostean O 2016 Issues regarding the modelling and simulation of hybrid micro grid systems *IOP Conf. Series: Materials Science and Engineering*. **106** pp. 1-5.
- [10] Rashid Al B, Mohammad A and Tapas M 2015 Speed control of synchronous machine by changing duty cycle of DC/DC buck converter *AIMS Energy*. **3** pp. 728-739.
- [11] Binayak B, Kyung-Tae L, Gil-Yong L, Young-Man C and Sung-Hoon A 2015 Optimization of Hybrid Renewable Energy Power Systems: A Review *International Journal of Precision Engineering and Manufacturing-Green Technology*. **2** pp. 99-112.
- [12] Rajesh K, Kulkarni A.D and Ananthapadmanabha T 2015 Modeling and Simulation of Solar PV and DFIG Based Wind Hybrid System *Procedia Technology*. **21** pp. 667 – 675.
- [13] Rajan singaravel M.M and Arul daniel S 2015 MPPT With Single DC-DC Converter and Inverter for Grid-Connected Hybrid Wind-Driven PMSG-PV System *IEEE Transactions on Industrial Electronics*. **62** pp. 4849-57.
- [14] Nahidul hoque S, Norhafizan A, Imtiaz ahmed C and Zahari T 2015 Technical Study of a Standalone Photovoltaic-Wind Energy Based Hybrid Power Supply Systems for Island Electrification in Malaysia, DOI:10.1371/journal.pone.0130678 June 29, 2015.
- [15] Bogaraj T, Kanakaraj J and Chelladurai J 2015 Modeling and simulation of stand-alone hybrid power system with fuzzy MPPT for remote load application *Archives of Electrical Engineering*. **64** pp. 487-504.
- [16] Sajib C Design and Analysis of a Hybrid Solar-Wind Energy System Using CUK & SEPIC Converters for Grid Connected Inverter Application *Journal of Electrical Engineering*. pp.1-7.
- [17] Barsana banu J , Balasingh moses M and Rajarajacholan S A non isolated bidirectional DC-DC converter with LCD snubber *Revista tecnica de la facultad de ingenieria universidad del zulia*. **39** pp.131-143.